SIR Publishers
CENTER FOR INTERNATIONAL SCIENTIFIC PUBLICATIONS
JOURNAL OF MULTIDISCIPLINARY BULLETIN
ISSN(Online): 2984-6722
SJIF Impact Factor |(2023): 5.887|
Volume-7, Issue-1, Published |20-01-2024|

COBALT FISCHER–TROPSCH CATALYST REGENERATION

https://doi.org/10.5281/zenodo.10491827

B.M.Abdullaev
Karshi Engineering Economic Institute
T.Kh.Sayfullaev
Karshi Engineering Economic Institute

ANNOTATION

Redispersion of cobalt is a key process in Fischer-Tropsch catalyst regeneration. Using model catalysts, we show that redispersion is a two-step process. Oxidation of supported metallic cobalt nanoparticles produces hollow oxide particles by the Kirkendall effect; reduction causes the disintegration of these hollow oxide shells and produces several metal particles. This mechanism is largely independent of support.

Keywords

Catalyst regeneration, Fischer–Tropschsynthesis · Kirkendall effect, cobalt nanoparticles

1.Introduction: Supported cobalt is the catalyst of choice for the gas-to-liquid (GTL) Fischer–Tropsch synthesis (FTS) step due to its high activity and selectivity toward straight-chain paraffins. Due to the cost of cobalt and precious metals, which are often used as promoters, the catalyst lifetime is required to make the process economically feasible. In addition to the relatively stable new catalyst synthesis regeneration can be used to extend the lifetime of Co FTS catalysts. A fundamental understanding of the deactivation mechanisms during FTS is key to designing an efficient regeneration process. Over the past 15 years, most of the research on cobalt catalyst deactivation has focused on oxidation as a deactivation mechanism. Our previous work showed that oxidation is not a deactivation mechanism during FTS for supported Co-catalysts with crystallite sizes larger than 2 nm. On the contrary, it was found that the FT environment strongly decreased. After a comprehensive study of cobalt catalyst deactivation under real FTS conditions, the following intrinsic deactivation mechanisms were identified: (1) Co active phase sintering (2) carbon deposition and (3) possible surface reconstruction. After identifying these mechanisms, a three-step regeneration process, i.e. (1) dewaxing (2) oxidation and (3) reduction, synthesis occurring during FTS was designed to reverse carbon deposition and surface regeneration. . The oxidation step was found to be crucial in burning harmful carbon and redistributing cobalt.

SIR Publishers
CENTER FOR INTERNATIONAL SCIENTIFIC PUBLICATIONS
JOURNAL OF MULTIDISCIPLINARY BULLETIN
ISSN(Online): 2984-6722
SJIF Impact Factor |(2023): 5.887|
Volume-7, Issue-1, Published |20-01-2024|

To date, there is little understanding of the mechanism of Co redistribution during regeneration. This understanding is crucial in the design and improvement of catalyst regeneration. The following article aims to shed light on the recovery mechanism during regeneration for an alumina supported catalyst. Due to the complexity of the real catalyst, model systems have been used to gain a deeper understanding of the redistribution mechanism in the regeneration process.

For the cobalt phase to redistribute, the cobalt must be clearly mobile from the location of the original particle. We used planar model catalysts (silica and alumina) consistent with TEM imaging, as well as a non-porous α-alumina supported model catalyst. The flat model system provides excellent contrast in TEM and allows us to find almost all cobalt. In addition, the sample can be subjected to subsequent reconstruction after imaging, after which the same sample area can be imaged again. It is an excellent tool to study morphological changes at the individual particle level and to study cobalt transport phenomena on the support in detail. By changing the support, its effect can also be studied. The use of α-alumina as a support is closer to a real catalyst support, but the absence of a pore structure allows for easier interpretation of TEM images. Another advantage of this catalyst model is that it can be characterized by standard catalyst characterization techniques such as X-ray diffraction.

2. Experiments

2.1 Flat model systems

More information about flat model support can be found elsewhere. Briefly, the sample consists of a cream wafer coated with a 15 nm thick silicon nitride membrane terminated by a 3 nm thick silicon oxide layer. At the center of the sample, a small portion of the underlying silicon wafer is etched away, leaving only the membrane thin enough to facilitate TEM imaging. A flat alumina support was formed by depositing c-alumina on a silica sample. SEM, AFM, and XPS analyzes showed a continuum 5 nm thick alumina layer, 1 nm roughness, similar to silica substrate. The Auger parameter of alumina (1461 eV) is between amorphous alumina and c-alumina. When the membrane breaks, it tends to fold, which provides a side view of the support surface that provides information about the z-coordinate of the sample. Cobalt was deposited by spin coating of a nitrate solution. A polymer (PMVE) was added to the spin coating solution, which mainly serves to increase the viscosity of the spin coating solution. The spincoating solution was prepared using a solution of 20 g of 25% PMVE in water to which 3 g of isopropanol was added. 0.5 mL of 65 mM cobalt nitrate solution was added to 5 mL of PMVE/water/isopropanol mixture, resulting in a cobalt concentration of 5.9 mM. For alumina-supported samples, a small amount of Pt was added in the form of platinum ammonium nitrate, which serves as a reduction promoter. The

SIR Publishers
CENTER FOR INTERNATIONAL SCIENTIFIC PUBLICATIONS
JOURNAL OF MULTIDISCIPLINARY BULLETIN
ISSN(Online): 2984-6722
SJIF Impact Factor |(2023): 5.887|
Volume-7, Issue-1, Published |20-01-2024|

concentration of Pt in the spincoating solution was 4.5 μM, i.e. the ratio of Co:Pt was 1.32:1. After spin coating, the samples were calcined at 350 °C (5 °C/min, 20% O2 in Ar) for 3 h, during which the cobalt nitrate was converted to cobalt oxide (Co3O4) and the polymer burned off (confirmed by XPS).). Stay again the same temperature program and gas composition were used in the oxidation steps. The reduction was carried out at 425 °C (2 °C/min, 4 h), in pure H2. After cooling to room temperature in hydrogen, the samples were passivated under controlled air exposure.

XPS is measured with a Kratos AXIS Ultra spectrometer equipped with a monochromatic Al K α X-ray source, a twin anode source (Al and Mg) and a delay line detector (DLD). Spectra were obtained using an aluminum anode (Al Ka = 1486.6 eV) operating at 150 W. Binding energies are tuned to the Si 2p peak of amorphous silicon at 103.3 eV. The Auger parameter of the alumina layer is determined using the Al anode of the twin source, where bremsstrahlung is responsible for the Al KL23L23 Auger peaks. TEM studies were performed on a Tecnai 20 (FEI Co.) operating at 200 kV. For XPS and TEM measurements, samples were exposed to air before measurements.

2.2 α-alumina supported model systems

Ceralox APA-0.5 (α-alumina, surface area 8 m2/g,) was impregnated with an aqueous cobalt nitrate solution of appropriate concentration to produce 10 wt% cobalt on the alumina model catalyst. After vacuum drying at 75-85°C, the sample was calcined in a fluidized bed in air at 250°C (1°C/min, 6 hours). Reduction was performed in pure hydrogen at 425 °C (1 °C/min, 10 h), followed by passivation on dry ice under an inert atmosphere. Controlled exposure to air creates a 3 nm CoO passivation layer that protects the particles from further oxidation. XRD measurements were performed using a Philips X'Pert Pro multipurpose diffractometer equipped with a Co Kα source. Average Co3O4 particle sizes were obtained by the full pattern refinement procedure. TEM measurements were performed on a JEOL 2010 microscope equipped with a LaB6 filament and operating at 200 kV.

3 Results

3.1 Co/SiO_2

After spincoating, calcination, and reduction, a typical silicon-supported planar model sample contains metallic cobalt particles coated with a 3 nm-thick CoO passivation layer. This was confirmed by XPS analysis, which revealed a mixture of metallic Co and CoO. Figure 1(a) shows the TEM image of the reduced sample. Particles of different sizes ranging from 30 nm to 3 nm in diameter are observed.

SIR Publishers
CENTER FOR INTERNATIONAL SCIENTIFIC PUBLICATIONS
JOURNAL OF MULTIDISCIPLINARY BULLETIN
ISSN(Online): 2984-6722
SJIF Impact Factor |(2023): 5.887|
Volume-7, Issue-1, Published |20-01-2024|

Oxidation of (passivated) metallic cobalt particles leads to dramatic morphological changes (Fig. 1b).

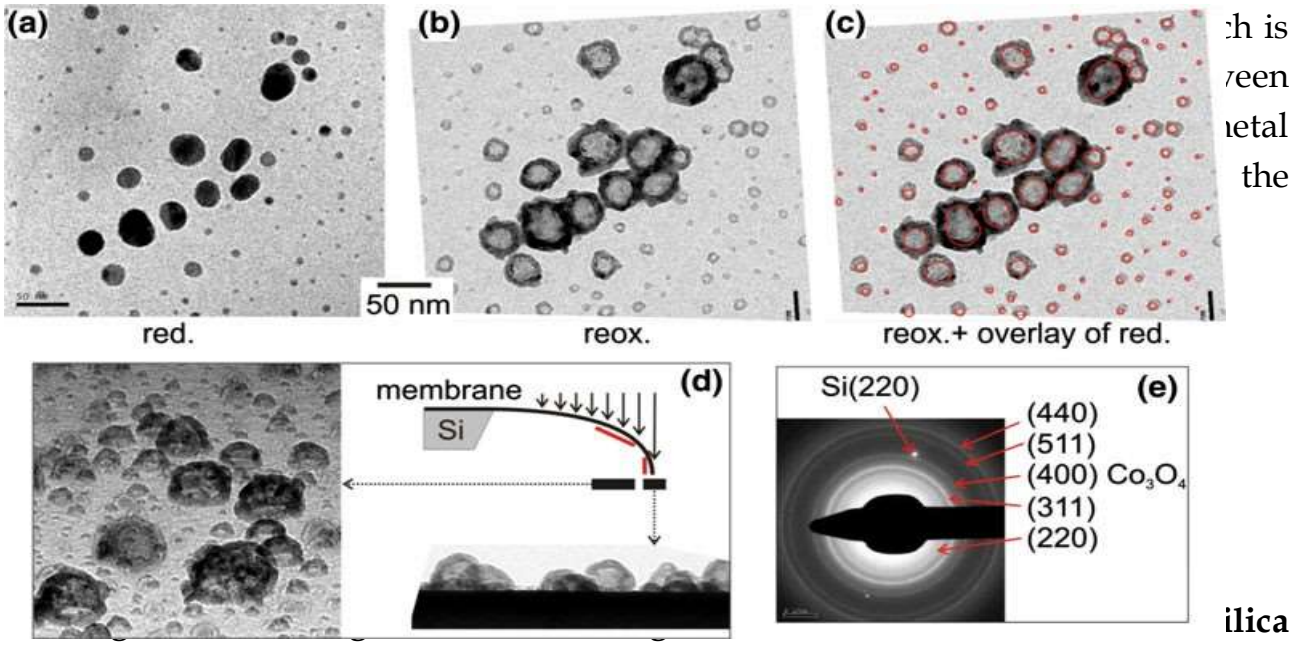

ilica support, showing the same sample area before and after reoxidation. In the panel (c) outline and position of the original metallic particles is indicated, on top of the reoxidized picture to facilitate detailed comparison. A broken membrane curls up and in this way images with a tilted membrane can be obtained, including a side view of the membrane (d). These images confirm that the hollow particles are closed on the top. e Electron diffraction shows diffuse diffraction rings typical of polycrystalline Co3O4

i.e., the hollow particles were the original metal particle. centered in place and not moving on the support. (2) The inner diameter of the hollow oxide particle is equal to the size of the original metal particle. (3) The same process occurs for different particle sizes.

Images of the tilt of the membrane relative to the electron beam (up to 90°, creating a side view) provide information about the z-direction of the sample. These images (Fig. 2d) clearly show that the hollow particles are closed at the top, so they are most clearly depicted as hollow (hemi-) spheres instead of donuts. Electron diffraction and XPS show that the hollow particles are composed of Co3O4. The Co 2p spectrum is identical to the Co3O4 reference. Silicate formation vs. link Co2? leads to an increase in the peaks associated with . Thus, we found no indication for silicate formation. The electron diffraction image (Fig. 2e) shows diffuse rings instead of more hidden spots, indicating that the oxide shell is highly polycrystalline, in agreement with the findings of other authors.

3.1.1 Redundancy

Figure 2 summarizes the results obtained after reducing the hollow oxide shells. This shows the same sample area in different redox stages. As can be seen

SIR Publishers
CENTER FOR INTERNATIONAL SCIENTIFIC PUBLICATIONS
JOURNAL OF MULTIDISCIPLINARY BULLETIN
ISSN(Online): 2984-6722
SJIF Impact Factor |(2023): 5.887|
Volume-7, Issue-1, Published |20-01-2024|

from these images, the redispersion of cobalt particles occurred after oxidation-reduction: the hollow oxide particles formed by oxidation are divided into several metallic cobalt particles during the reduction process. These particles form a ring-like structure on the support in the position of the original oxide shell. Thus, it is clear that regeneration leads to an increase in surface area, as one large metal particle is transformed into several smaller metal particles. All metallic cobalt particles were located where the oxide was present before oxidation, indicating that the mobility of cobalt on the support (sintering) was low when reduced at 425 °C.

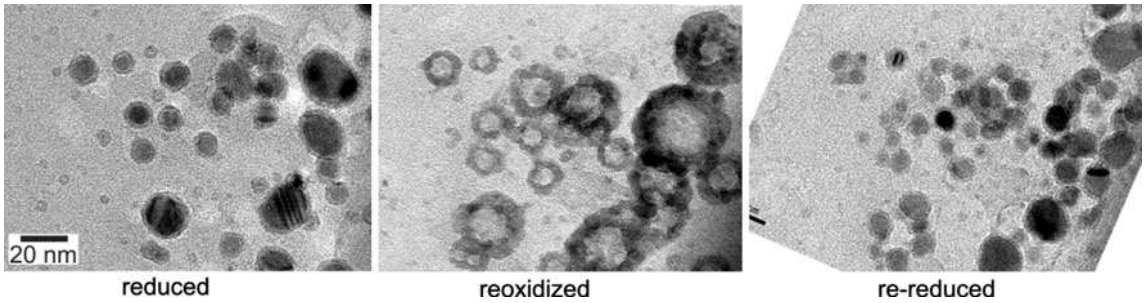

Figure 2. Bright field TEM images of the same sample area during the different steps of the oxidation–reduction treatment. It can be seen that reduction of the hollow particles leads to redispersion of the cobalt phase

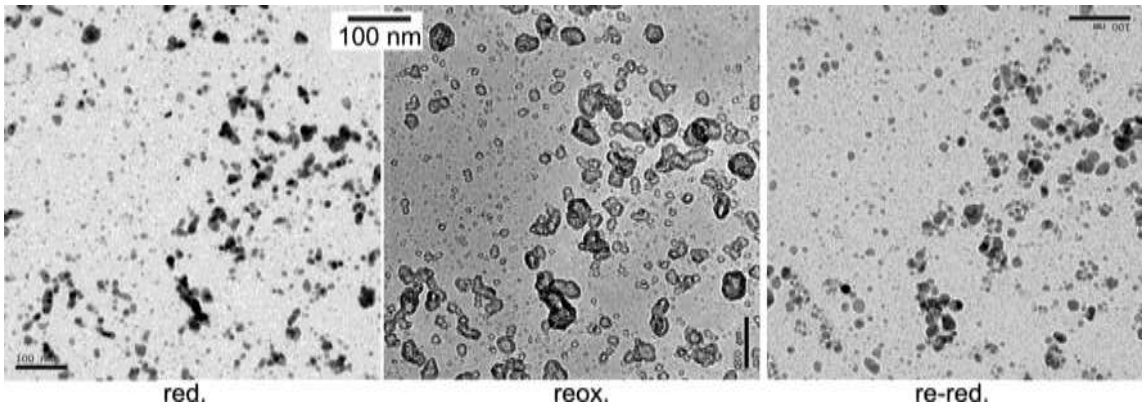

Figure 3. Bright field TEM images of a flat cobalt-on-alumina flat model catalyst, showing the reduced, reoxidized and re-reduced form of the same sample area. Hollow oxide particle are formed during oxidation, and they break up during reduction, similar to the silica system

3.2 Co/Al_2O_3

The role of the support was investigated using a model alumina support instead of silicon. The results of this study are summarized in Figure 3. Alumina is a more reactive support, making reduction of alumina-supported cobalt more difficult in general. It is difficult to measure the degree of reduction directly from our samples, and the effect of the support appears to be mostly indirect: the metal particles on alumina appear more irregular and the larger agglomerates are full, in contrast to the silica samples. does not appear to be distinct. Figure 1. We tentatively explain this by the incomplete reduction of cobalt oxide supported by alumina. In this paper, we focus only on the effect of aid on the redistribution

SIR Publishers
CENTER FOR INTERNATIONAL SCIENTIFIC PUBLICATIONS
JOURNAL OF MULTIDISCIPLINARY BULLETIN
ISSN(Online): 2984-6722
SJIF Impact Factor |(2023): 5.887|
Volume-7, Issue-1, Published |20-01-2024|

process. The re-oxidation of the alumina-supported sample similar to that of the silica sample leads to the formation of hollow oxide particles, and the reduction of hollow particles indicates the decomposition of the hollow oxide particles. Although the results for flat alumina are not clear, its nature is clearsupport does not fundamentally change the backscattering mechanism found on the silica support.

3.2.1 α-Alumina Supported Model Systems

A study of cobalt supported on nonporous α-alumina revealed a similar redistribution mechanism. In this paper, we show only a small part of the work, just to show that the flat model work can be extended to more realistic supported systems. A full report on this case will be published elsewhere. Figure 4 shows the TEM images of the α-alumina-supported cobalt catalyst at different stages of the reduction-oxidation-reduction procedure. A sample in the reoxidized phase (center image) shows the formation of hollow oxide particles. Comparing the reduced state before and after oxidation, it is clear that the larger cobalt particles have completely disappeared and instead a large number of small cobalt crystallites appear. XRD was carried out in the calcined and reoxidized state. Average Co3O4 particle diameter in a fresh sample before the first reduction step is 30 nm, and the average particle size in the reoxidized sample is 9 nm. This smaller XRD particle size in the reoxidized state can be rationalized by the special morphology in the reoxidized state: cobalt oxide exists as hollow polycrystalline particles, and XRD only determines the average size of the individual crystallites that make up the crystal. hollow oxide shell. We found no indication of aluminate formation in any of the alumina model catalysts.

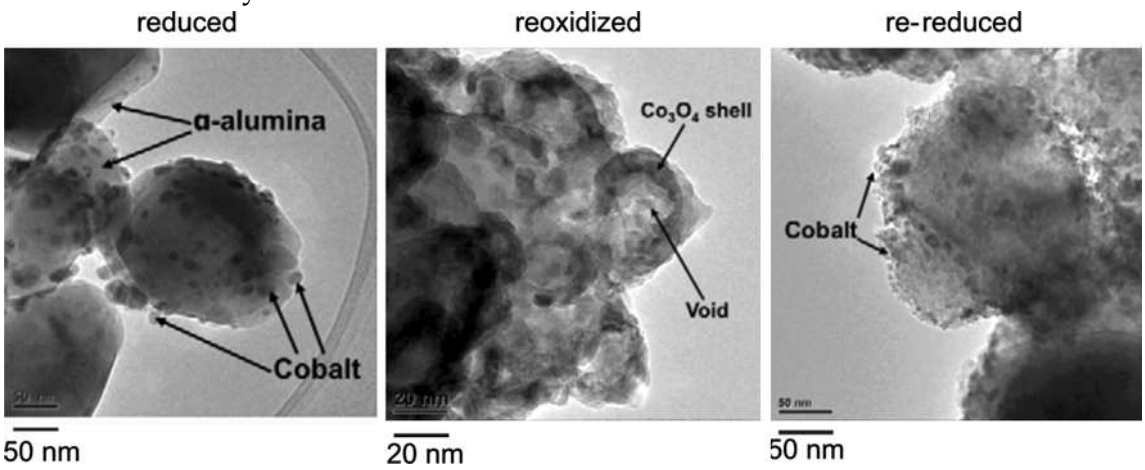

Figure 4. Bright field TEM images of a *a*-alumina-supported cobalt model catalyst, showing the formation of hollow oxide spheres in the reoxidized stage and higher metallic cobalt dispersion in the re-reduced state

4 Discussion

SIR Publishers
CENTER FOR INTERNATIONAL SCIENTIFIC PUBLICATIONS
JOURNAL OF MULTIDISCIPLINARY BULLETIN
ISSN(Online): 2984-6722
SJIF Impact Factor |(2023): 5.887|
Volume-7, Issue-1, Published |20-01-2024|

Spent alumina-supported FT catalyst can be regenerated using a procedure that involves solvent washing to remove excess wax, oxidation to remove residual carbon and redispersion of cobalt, followed by hydrogen-assisted reactivation. Our model systems of varying degrees of complexity capture the essential elements of spent FT catalyst after dewaxing: the samples have high degradation rates similar to those found for spent samples. Our samples contain both large and small particles, thus simulating a sintered catalyst. This makes our findings on model systems highly relevant for understanding the processes occurring during real cobalt FT catalyst regeneration.

The mobility of cobalt on the support is a crucial parameter in the redistribution of cobalt. During FT synthesis, an initially well-dispersed metal system tends to sinter, an inevitable process controlled by thermodynamics. The gas atmosphere can have a strong effect on the sintering kinetics, i.e., the mobility of cobalt, e.g. Reversal of sintering, redispersion requires a mechanism that promotes the dispersion of the cobalt phase. In almost all cobalt-visible flat model samples, the mobility of cobalt on the support was found to be low during oxidation and reduction. The only significant mobility of cobalt on the support observed in our experiments is limited by the formation of hollow oxide shells during the oxidation of metal particles. This is also the type of mobility required for redistribution: cobalt is transported away from its original location.

The formation of hollow oxide particles by oxidation has been previously reported, including Co, Ni, Fe, Cu and the mechanism responsible for this is the Kirkendall effect, where diffusion differences exist. reactants in solid-state reactions lead to cavity formation. In the oxidation of metal nanoparticles, the diffusion of metal (cations) out through the growing oxide layer is much faster than the inward diffusion of oxygen. Thus, the oxide layer grows outward, eventually forming a hollow oxide particle. In our special system, the size of the internal cavity equal to the size of the original metal particle, meaning oxygen diffusion is negligible. Cobalt mobility must be low during reduction to avoid complete redistribution of cobalt due to the Kirkendall effect. After pulling back, we observe exactly this: instead of collapsing into a single metal particle, the hollow shells disintegrate to form several smaller metallic cobalt particles in place of the original cobalt oxide shell.

The precise nature of the aid does not fundamentally alter redistribution through the Kirkendall mechanism. The planar model systems of silica and alumina and the more realistic model system of the α-alumina support show the same redistribution mechanism. The formation of hollow cobalt oxide particles for Co supported on montmorillonite supports the idea that the Kirkendall effect is a

JOURNAL OF MULTIDISCIPLINARY BULLETIN
ISSN(Online): 2984-6722
SJIF Impact Factor |(2023): 5.887|
Volume-7, Issue-1, Published |20-01-2024|

general mechanism that occurs on any type of support. Thus, a similar redispersion mechanism can be expected in a real FT catalyst.

5. Conclusion

We used model cobalt catalysts to study the redistribution mechanism of cobalt during redox treatment. Metallic cobalt is oxidized by the formation of hollow oxide particles, the size of which is the same as the original metal particle. Thus, cobalt moves away from its original state during the oxidation process, which is an important first step for the redistribution of cobalt. The second stage of re-dispersion occurs during the reduction of hollow particles: they are divided into several smaller cobalt particles, which are located in a ring in the position of the original oxide shell. Since cobalt transport via the Kirkendall mechanism is the only source of cobalt mobility on the support, we conclude that this mechanism is a crucial component of catalyst regeneration. This redistribution mechanism is largely independent of the support and thus it is responsible for the redistribution of cobalt during the regeneration of the real FT catalyst.

LIST OF USED LITERATURE:

1. D. Tailor, Field Joint Developments and Compatibility Considerations,ResearchGate, October 2003.
2. Journal of Protective Coatings and Linings, Protecting and Maintaining Transmission Pipeline, Technology Publishing Company, Pittsburgh, 2012.
3. Coaltarenamel, PCI International (May 31,2001). http://www.pcimag.com/articles/85670-coal-tar-enamel.
4. K. Andre, The use of coal tar enamel for lining and wrapping pipes, TheCivil Engineer 9(1) (January 1967) 1e8.
5. T. Rehberg, M. Schad, Corrosion protective coating technology for transitpipelines in Europe, in: 3R International, February 2010.
6. DENSOLEN®-AS40 Plus,[Online].Available: http://www.denso.de/en/products/product/densolen-pebutyl-tapes-and-mastics/densolen-corrosion-prevention-tape-three-ply/densolen-as40-plus/.
7. Rizayev, S. A., Abdullayev, B. M., & Jumaboyev, B. O. (2023). GAZLARNI KIMYOVIY ARALASHMALARDAN TOZALASH JARAYONINI TADQIQ QILISH. *Sanoatda raqamli texnologiyalar/Цифровые технологии в промышленности*, *1*(1), 71-75.
8. Mengliqul o'g'li, A. B. (2022). NANOO 'LCHAMLI KATALIZATORLAR OLISH VA ULARNI OLEFINLARNI GIDROGENLASHDA

QO ‘LLASH. *O'ZBEKISTONDA FANLARARO INNOVATSIYALAR VA ILMIY TADQIQOTLAR JURNALI*, *2*(14), 854-858.

9. Rizayev, S., & Abdullayev, B. (2022). ETILEN ASOSIDA BENZOL OLISH VA UNI SANOATDA ERITUVCHI SIFATIDA QO ‘LLASH. *Journal of Integrated Education and Research*, *1*(6), 99-102.

10. Абдуллаев, Б., & Анварова, И. (2022). ПОЛИЭТИЛЕН ИШЛАБ ЧИҚАРИШ ЛИНИЯСИДА СОВУТУВЧИ ТИЗИМ ҚУРУЛМАЛАРИНИ ТАКОМИНЛАШТИРИШ. *Journal of Integrated Education and Research*, *1*(6), 40-43.

11. Khudayorovich, R. D., Rizoevich, R. S., & Abdumalikovich, N. F. (2022). MODERN CATALYSTS FOR ACETYLENE HYDROCHLORATION. *Galaxy International Interdisciplinary Research Journal*, *10*(2), 27-30.

12. Abdullayev, K. O. A. I. (2023). RESEARCH OF THE CATALYTIC PROPERTIES OF A CATALYST SELECTED FOR THE PRODUCTION OF HIGH-MOLECULAR WEIGHT LIQUID SYNTHETIC HYDROCARBONS FROM SYNTHESIS GAS. *Химическая технология*, *14*(10), 115.

13. Mengliqul o’g’li, A. B. (2022). NANOO ‘LCHAMLI KATALIZATORLAR OLISH VA ULARNI OLEFINLARNI GIDROGENLASHDA QO ‘LLASH. *O'ZBEKISTONDA FANLARARO INNOVATSIYALAR VA ILMIY TADQIQOTLAR JURNALI*, *2*(14), 854-858.

14. ANALYSIS OF THE CAUSES OF ACCIDENTS IN GAS PIPELINES TRANSPORT, NATIONAL ECONOMY AND MAIN PIPELINES

15. Torayevich, K. M. (2023). DETERMINATION OF THE INFLUENCE OF THE COMPOSITION OF CATALYSTS ON THE CATALYTIC CHARACTERISTICS. *JOURNAL OF MULTIDISCIPLINARY BULLETIN*, *6*(5), 8-15.

16. Torayevich, K. M. (2023). DEVELOPMENT OF HYBRID CATALYST AND SYNTHESIS OF LIQUID HYDROCARBONS BASED ON THEM. *JOURNAL OF MULTIDISCIPLINARY BULLETIN*, *6*(5), 1-7.

17. Karshiev, M. T., Kh, S. T., & Abdullaev, B. M. (2023). PURIFICATION OF NATURAL GAS FROM CO2 BY ADSORPTION METHOD. *JOURNAL OF MULTIDISCIPLINARY BULLETIN*, *6*(5), 62-76.

18. Xayrulla o‘g‘li, S. T. (2022). YO‘LDOSH GAZLARNI QAYTA ISHLASH ZAVODLARIDAGI KORROZIYA BILAN BOG‘LIQ MUAMMOLARNI YECHISHDA INGIBITORLARDAN FOYDALANISH. *Journal of new century innovations*, *10*(4), 20-22.

19. Rahmatovich, C. N., & Xayrulla o‘g‘li, S. T. (2022). YO‘LDOSH GAZ-KONDENSATLARINI BARQARORLASHTIRISH QURILMALARIDA INGIBITORLARDAN FOYDALANISH. *Journal of new century innovations*, *10*(4), 23-25